Acta Oceanol. Sin., 2023, Vol. 42, No. 2, P. 120–133
https://doi.org/10.1007/s13131-022-2125-y
http://www.aosocean.com
E-mail: ocean2@hyxb.org.cn

Sedimentary characteristics and genetic mechanism of the giant ancient pockmarks in the Qiongdongnan Basin, northern South China Sea

Pengfei Xiong[1, 2, 3], Cong Cheng[1], Zenggui Kuang[2]*, Jinfeng Ren[2], Jinqiang Liang[2], Hongfei Lai[2], Zigui Chen[1], Jiang Lu[3], Xiaoyu Fang[3], Tao Jiang[1]*

[1] Hubei Key Laboratory of Marine Geological Resources, China University of Geosciences, Wuhan 430074, China

[2] Guangzhou Marine Geological Survey, Ministry of Natural Resources, Guangzhou 510075, China

[3] Southern Marine Science and Engineering Guangdong Laboratory (Zhanjiang), Zhanjiang 524088, China

Received 23 June 2022; accepted 11 October 2022

Abstract

In the late Miocene, giant ancient pockmarks, which are fairly rare globally, developed in the Qiongdongnan Basin. In this paper, to determine the sedimentary characteristics and genetic mechanism of these giant ancient pockmarks in the Yinggehai Formation of the Qiongdongnan Basin, based on high-resolution 3D seismic data and multiattribute fusion technologies, we analyzed the planar distribution and seismic facies of the ancient pockmarks and compared the characteristics of the ancient pockmarks with those of channels, craters, and hydrate pits. Moreover, we also discussed the implications of the fluid escape system and paleo-bottom current activity in the ancient pockmark development area and analyzed the influence of the ancient pockmarks on the paleoclimate in this region. Finally, an evolutionary model was proposed for the giant ancient pockmarks. This model shows that the giant ancient pockmarks in the southern Qiongdongnan Basin were affected by both deep fluid escape and lateral transformation of paleobottom currents. In addition, the giant ancient pockmarks contributed to the atmospheric CO_2 concentration in the late Miocene and played a great role in the contemporary evaluation of deepwater petroleum exploration.

Key words: giant ancient pockmark, bottom current, fluid escape, Yinggehai Formation, Qiongdongnan Basin

Citation: Xiong Pengfei, Cheng Cong, Kuang Zenggui, Ren Jinfeng, Liang Jinqiang, Lai Hongfei, Chen Zigui, Lu Jiang, Fang Xiaoyu, Jiang Tao. 2023. Sedimentary characteristics and genetic mechanism of the giant ancient pockmarks in the Qiongdongnan Basin, northern South China Sea. Acta Oceanologica Sinica, 42(2): 120–133, doi: 10.1007/s13131-022-2125-y

1 Introduction

The escape of fluids in deep seabed formations may lead to the release of large amounts of greenhouse gases and may even induce marine geological disasters caused by instabilities in the seabed topography, thus indirectly affecting the environment, oil-gas resources, and marine engineering (Davy et al., 2010; Sun et al., 2011; Zhu et al., 2021). Submarine pockmarks have been widely studied because they are a sign of deep-formation fluids escaping on the seafloor (Sun et al., 2011; Hovland and Sommerville, 1985; Hovland et al., 2002; Judd and Hovland, 2007; Böttner et al., 2019). As early as 1970, King and Maclean, famous geologists, discovered the existence of seabed pockmarks on the continental shelf of Nova Scotia, Canada, and carried out research from the perspectives of topography and sedimentary facies. However, due to the lack of high-precision seismic data and analytical technologies at that time, the genetic mechanism of the pockmarks was not effectively confirmed (King and Maclean, 1970). It was not until 1985 that Hovland et al. analyzed gas composition data obtained in the subsea pockmark development area and proved that the pockmarks are depression landforms formed by the upward movement of deep fluids through migration pathways and that these fluids were released on the seafloor (Hovland and Sommerville, 1985). With continuous innovations in seismic exploration technologies, geologists have obtained a further understanding of pockmarks. Pockmarks have been confirmed to develop in estuaries, on continental shelves, on continental slopes, and on abyssal plains (Böttner et al., 2019; Sun et al., 2011; Luo et al., 2012). Hovland et al. divided pockmarks into 6 types, including unit, chain, and compound pockmarks, according to their planar distribution characteristics and scale (Hovland et al., 2002). Regarding their planar distribution, pockmarks often appear as crescents, ellipses, chains, or slender shapes while appearing in V, U, or W shapes in the seismic section (Judd and Hovland, 2007). Previous studies have shown that most pockmarks are between 10 m and 200 m in diameter (Sun et al., 2011; Luo et al., 2012), with some reaching far beyond this size. Pilcher and Argent (2007) coined the term "giant pockmarks" to describe pockmarks larger than 1 000 m in diameter. A giant pockmark with a diameter of more than 10 km has developed on the seabed of the Chatham Uplift in New Zealand (Davy et al., 2010); this pockmark is the largest found in the world thus far.

Geologists used sonar and multibeam technologies to suc-

Foundation item: The National Natural Science Foundation of China under contract No. 41976073; the Guangdong Major Project of Basic and Applied Basic Research under contract No. 2020B0301030003; the Southern Marine Science and Engineering Guangdong Laboratory (Zhanjiang) Project under contract No. ZJW-2019-03; the China Geological Survey Project under contract No. DD20190230.
*Corresponding author, E-mail: kzg21001@163.com; taojiang@cug.edu.cn

cessively discover submarine pockmarks on the northern continental margin of the South China Sea (Liang et al., 2017; Sun et al., 2011; Lin, 1995). However, studies using these technologies are often limited with regard to the dimensional accuracy of the analyzed pockmarks (Zhu et al., 2021). High-precision 3D seismic data have great advantages in revealing seabed pockmarks (Wang et al., 2011; Lu et al., 2017). Based on past analytical results obtained for seismic profiles and derived seafloor pore water geochemical test data, pockmarks can be divided into two types: the active type (Liu et al., 2017) and the inactive type (Sun et al., 2018; Guan et al., 2014). The submarine fluid in the northern part of the South China Sea is active, so submarine pockmarks are actively developing in this region (Guan et al., 2014; Zhu et al., 2021). Presently, submarine pockmarks with obvious scales have been discovered in the Zhujiang River Mouth Basin (Liu et al., 2017), Qiongdongnan Basin, Zhongjiannan Basin (Sun et al., 2011; Bai et al., 2014; Geng et al., 2017; Chen et al., 2018), Xisha Uplift (Guan et al., 2014), and Liyue Basin (Zhang et al., 2019) in the southern South China Sea, some of which are even giant pockmarks (Sun et al., 2011; Chen et al., 2015; Zhang et al., 2020).

Previous studies have illustrated that the formation of seabed pockmarks is closely related to the escape of deep-formation fluids and the actions of seafloor-bottom currents (Hovland et al., 2002; Pilcher and Argent, 2007; Sun et al., 2011; Zhu et al., 2021). Pockmarks reflect vivid indications of tectonic activities, bottom current activities, sedimentary environment evolution mechanisms, and the exploration of oil-gas resources such as natural gas hydrates (Wang et al., 2011; Sun et al., 2018; Zhu et al., 2021). Although some achievements have been made in researching and understanding seabed pockmarks both in China and globally (Sun et al., 2017; Pilcher and Argent, 2007; Hovland and Sommerville, 1985; Hovland et al., 2002; King and Maclean, 1970; Böttner et al., 2019), few discoveries or studies on ancient pockmarks formed in geologically historical periods and buried under the seabed have been reported (Bai et al., 2014). In this research, we found that giant ancient pockmarks developed at the bottom of the Yinggehai Formation in the Qiongdongnan Basin, exemplifying globally rare landforms. Using high-precision 3D seismic data, we analyzed the planar distribution and seismic facies characteristics of these ancient pockmarks using multiattribute fusion technologies, compared the characteristics of the ancient pockmarks with those of channels and craters, and clarified the deposition mechanism of the ancient pockmarks. In addition, the genetic mechanism of the ancient pockmarks was revealed by combining the processes in which deep-formation fluid escapes and bottom currents cause erosion. We also discuss the influence of the studied ancient pockmarks on the paleoclimate, and the relevant sedimentary evolution processes. Researching these ancient pockmarks can not only serve researchers in further understanding the geomorphological characteristics of ancient pockmarks but can also provide a reference for analyses of sedimentary paleoenvironments.

2 Geological setting

The Qiongdongnan Basin is located in the northern part of the South China Sea, characterized by a Cenozoic rift basin that is NE trending overall and reflects the topographic features of being high in the northern and southern regions and low in the central area (Ren and Lei, 2011; Xie et al., 1996; Cheng et al., 2021; Sun et al., 2015). This basin is connected to the Yinggehai Basin in the west, the Hainan Uplift region in the north, the Zhujiang River Mouth Basin in the east, and the Yongle Uplift region in the south (Cheng et al., 2021; Su et al., 2009) (Fig. 1). The area of the basin is approximately 45 000 km^2, and the contemporary maximum water depth exceeds 3 000 m. Since the Miocene, most of this basin has exhibited a semideep-sea–deep-sea sedimentary environment (Xiong et al., 2021; Li et al., 2018c; Cheng et al., 2021). Bounded by the T60 breakup unconformity, the Qiongdongnan Basin can be divided into a lower rifting period and an upper depression period (Jiang et al., 2013; Ren and Lei, 2011; Xie et al., 1996; Wu et al., 2018) (Fig. 2). During the rifting period, the basin experienced strong tectonic activity, while in the depression period, which tended to be stable, the tectonic activity almost stopped (Cao et al., 2015; Su et al., 2009). In addition, according to the differences in the subsidence rate, the basin depression period can be divided into an early thermal subsidence period and a late accelerated subsidence period (Jiang et al., 2013; Ren and Lei, 2011; Xie et al., 1996). Drilling measurements have confirmed that several sets of source rock formations with good hydrocarbon generation potential exist in the basin, among which the Yacheng Formation coal measure is the main source rock (Wei et al., 2021; Lai et al., 2021; Fang et al., 2019).

The study area considered in this research is located in the southwest area of the Beijiao Sag in the southern Qiongdongnan Basin (Fig. 1), with an area of approximately 1 000 km^2 and a contemporary water depth of approximately 1 500 m. Drilling activities at YL19-1-1 have revealed that the Miocene strata in the Qiongdongnan Basin mainly comprise mudstones, with a large number of developed deep-sea muddy deposits (Lei and Ren, 2016; Li et al., 2021).

3 Data and methods

The application prospects of high-precision 3D seismic data and multiattribute fusion technologies have facilitated improved rigorous analyses of the shape, structure and genetic mechanisms of ancient pockmarks. Over the past few years, the Guangzhou Marine Geological Survey collected 2D and 3D seismic reflection data using a G gun type-II air gun. Among their data, 3D seismic data were acquired in 2018 with a main frequency range of 30–70 Hz, a sampling interval of 1 ms, and a bin size of 3.125 m (inline direction)×18.75 m (crossline direction). The seismic data used in this study were processed using the GeoCluster (a CGG® product) processing system applied by the Guangzhou Marine Geological Survey (Ye et al., 2018). Moreover, the sequential stratigraphic framework utilized herein was determined based on the study of Cheng et al. (2021) (Fig. 3). Second, the horizontal coherence slice attributes and time structure diagram of the T30 interface were extracted by Geoframe® software (a Schlumberger® product)(Figs 4b and 5). In addition, by combining Petrel® software (a Schlumberger® product) with the time–depth conversion formula provided by the Guangzhou Marine Geological Survey and calculating the denudation thickness using the sedimentation rate provided by the Guangzhou Marine Geological Survey, paleomorphological maps of Horizons T30 and T40 in the study area were drawn(Fig. 4a). Based on the features of paleogeomorphology and seismic profiles, we measured and obtained the three-dimensional characteristic data of ancient pockmarks in the study area (Table 1). The global CO_2 content data and change curves applied in this study were summarized by Wei and Tian (2022).

4 Results

4.1 *Planar characteristics of ancient giant pockmarks*

According to the recovered palaeomorphological information and extracted coherent attributes, during the depositional

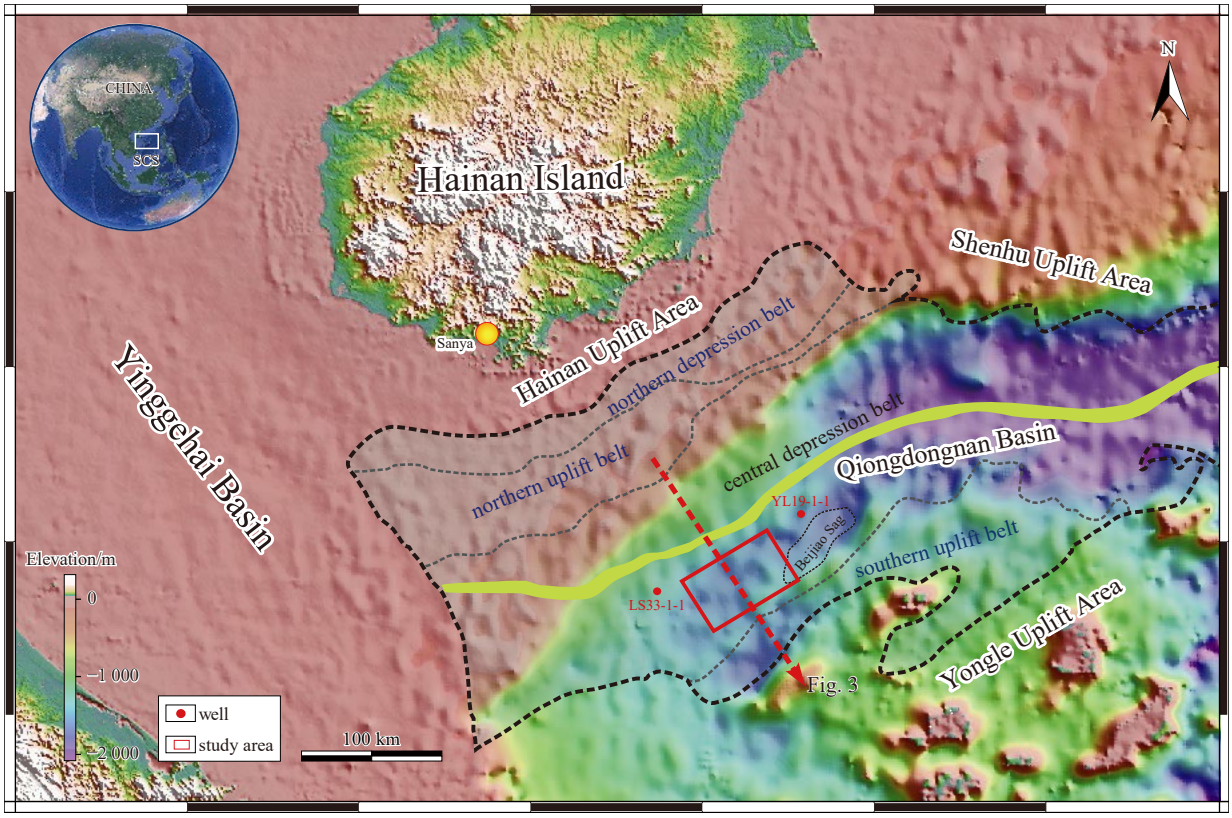

Fig. 1. Location of the study area (red rectangle) in the Qiongdongnan Basin (black dashed line boundary), northern South China Sea (insert) (modified from Lei and Ren (2016), Cao et al. (2015) and Jiang et al. (2013)). The elevation data were derived from Tozer et al. (2019). Moreover, the deep-water well data were derived from Lei and Ren (2016).

period of the Yinggehai Formation, ancient pockmarks were mainly distributed in the northern part of the study area and could be divided into oval-, crescent- and chain-shaped pockmarks according to their planar shapes (Fig. 4a). Among the identified pockmarks, nos 1–6 are fully developed in the study area. Except for pockmark no. 4, which is crescent-shaped, the rest are oval-shaped. Pockmark no. 4 is a crescent-shaped pockmark that protrudes southward on the plane (Figs 4a and 5). Pockmarks 7, 8, and 9 are incomplete in the study area. Pockmark nos. 7 and 8 are chain pockmarks, and no. 7 has chain branches. No. 9 is presumed to be an oval-shaped pockmark (Figs 4a and 5). In general, the strikes of pockmark nos. 4, 5, 7, 8, and 9 in the study area are nearly all east–west oriented, while the rest are nearly northeast-oriented (Figs 4a and 5). In addition, ancient pockmarks no. 3 and no. 9 developed multiple depression centers, and pockmark no. 5 is composed of two individual closely spaced but not connected pockmarks (Fig. 5). Among the six complete pockmarks identified in the study area, pockmark no. 1 is the largest, with a long-axis diameter of 4.95 km, a short-axis diameter of 2.21 km, and a depth of 0.34 km; pockmark no. 2 is the smallest in scale, with a long-axis diameter of 2.29 km, a short-axis diameter of 1.25 km, and a depth of 0.43 km; and pockmark no. 6 is the shallowest, with a depth of 0.33 km (Table 1). The pockmarks identified in the study area do not exhibit good symmetry, and the south/southeast side of the inner wall of the pockmarks are steeper than the other pockmark surfaces (Figs 4a and 5).

4.2 *Seismic reflection characteristics of giant ancient pockmarks*

According to the high-precision 3D seismic profile derived herein, the nine ancient pockmarks developed in the study area show obvious concave features and are either U-, V-, or W-shaped. The interiors of the ancient pockmarks are mainly filled with weak-amplitude sediments, with a small amount of medium-strong-amplitude sediments at the bottoms, and the south/southeast sides of the inner walls of the ancient pockmarks are steeper than the other pockmark surfaces (Table 1; Figs 4a and 5). No truncation reflections were observed in the strata developed in the ancient pockmarks in the study area. In the seismic section, the strata underlying the pockmarks show obvious pull-down or chaotic seismic reflection characteristics, and gas chimney structures and obvious strong-amplitude anomaly zones can be observed in some areas (Figs 4c and 6). In addition, a turbidite channel at the top of the Meishan Formation and mass transport deposits in the late depositional stage of the Yinggehai Formation can also be observed on the seismic profile in the study area (Fig. 6). The interior channel sediments mainly comprise channel sands, exhibiting strong amplitudes on the seismic profile. In the strata overlying the turbidite channel, obvious interlayer small faults can also be observed (Fig. 6).

4.3 *Characteristics of channels at the top of the Meishan Formation and MTDs of the late Yinggehai Formation*

In the late sedimentary period of the Yinggehai Formation, a large set of mass-transport deposits (MTDs) developed in the north and west of the study area (Fig. 7d), which showed obvious disorderly reflections on the seismic profile (Fig. 7e). The MTDs were supplied by a NW source and can cover most of the pockmarks in the study area. In the seismic profile between Horizons T40 and T27, an obvious interlayer fault can be identified, and

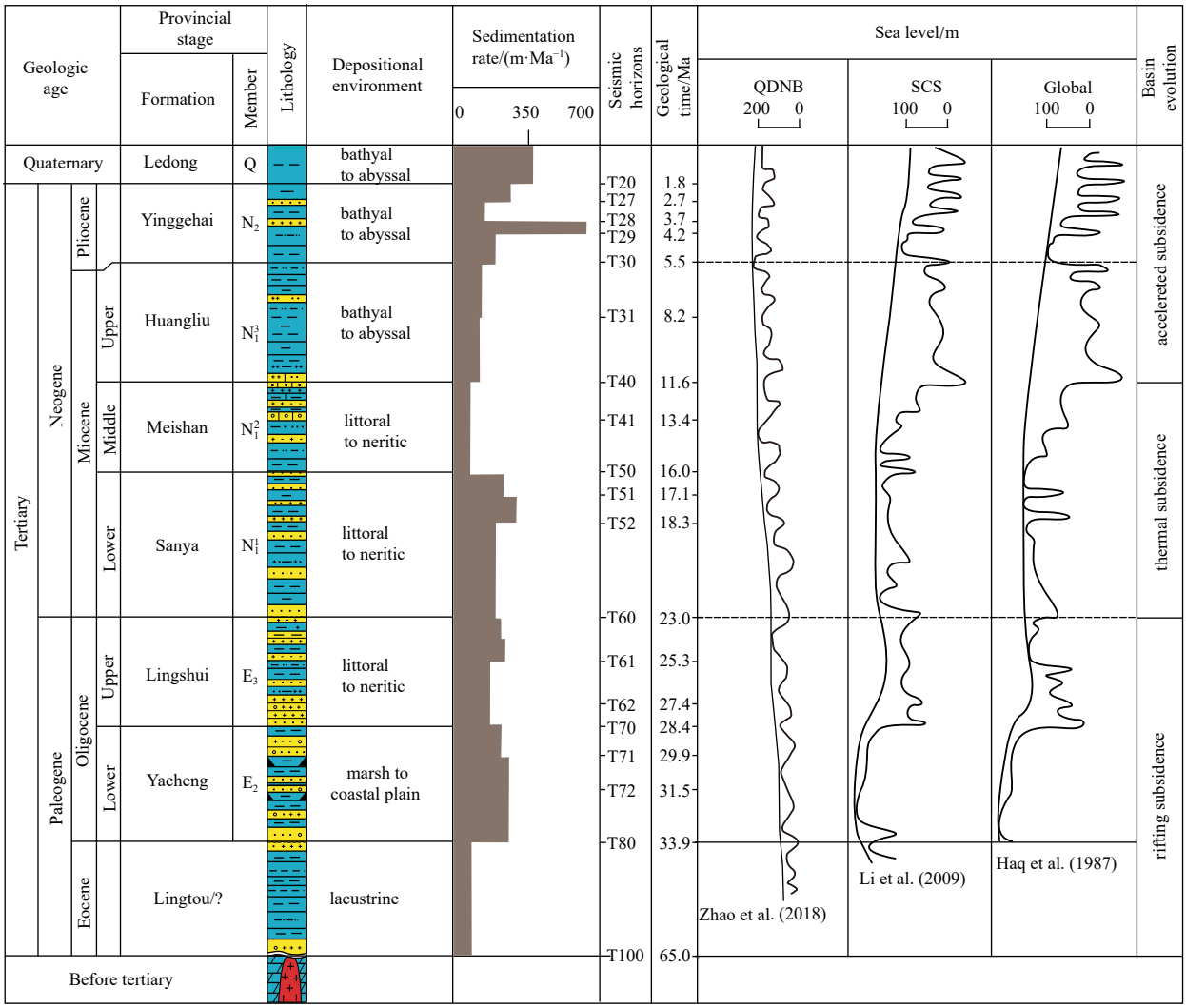

Fig. 2. Simplified stratigraphic, age, and lithological column information characterizing the Qiongdongnan Basin (modified from Jiang et al. (2013) and Cheng et al. (2021)). The sedimentation rate series was derived from Zhao et al. (2018). The sea level curves were derived from Zhao et al. (2018), Li (2009) and Haq et al. (1987).

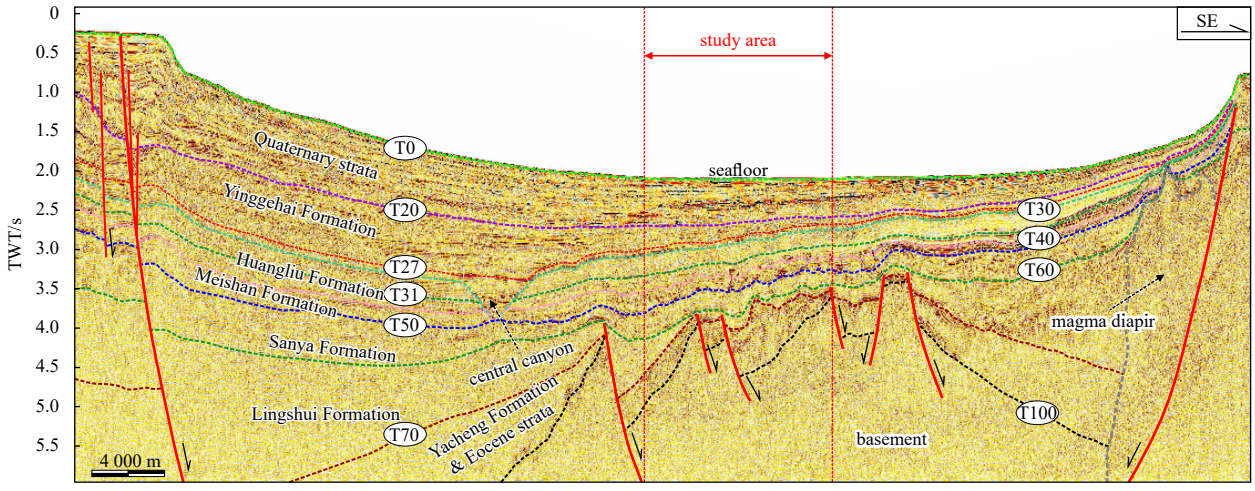

Fig. 3. Sequential stratigraphy of the Qiongdongnan Basin, modified from Cheng et al. (2021) (the section location is shown in Fig. 1).

some even run through the T30 interface but not through the T27 interface (Fig. 7e). On the top of the Meishan Formation, large-scale channel sediments developed in the study area, which showed strong amplitude bands on the RMS attribute map (Fig. 7b). In the seismic profile, the channel sedimentary body is mainly filled with weak amplitude deposition, which is U-shaped

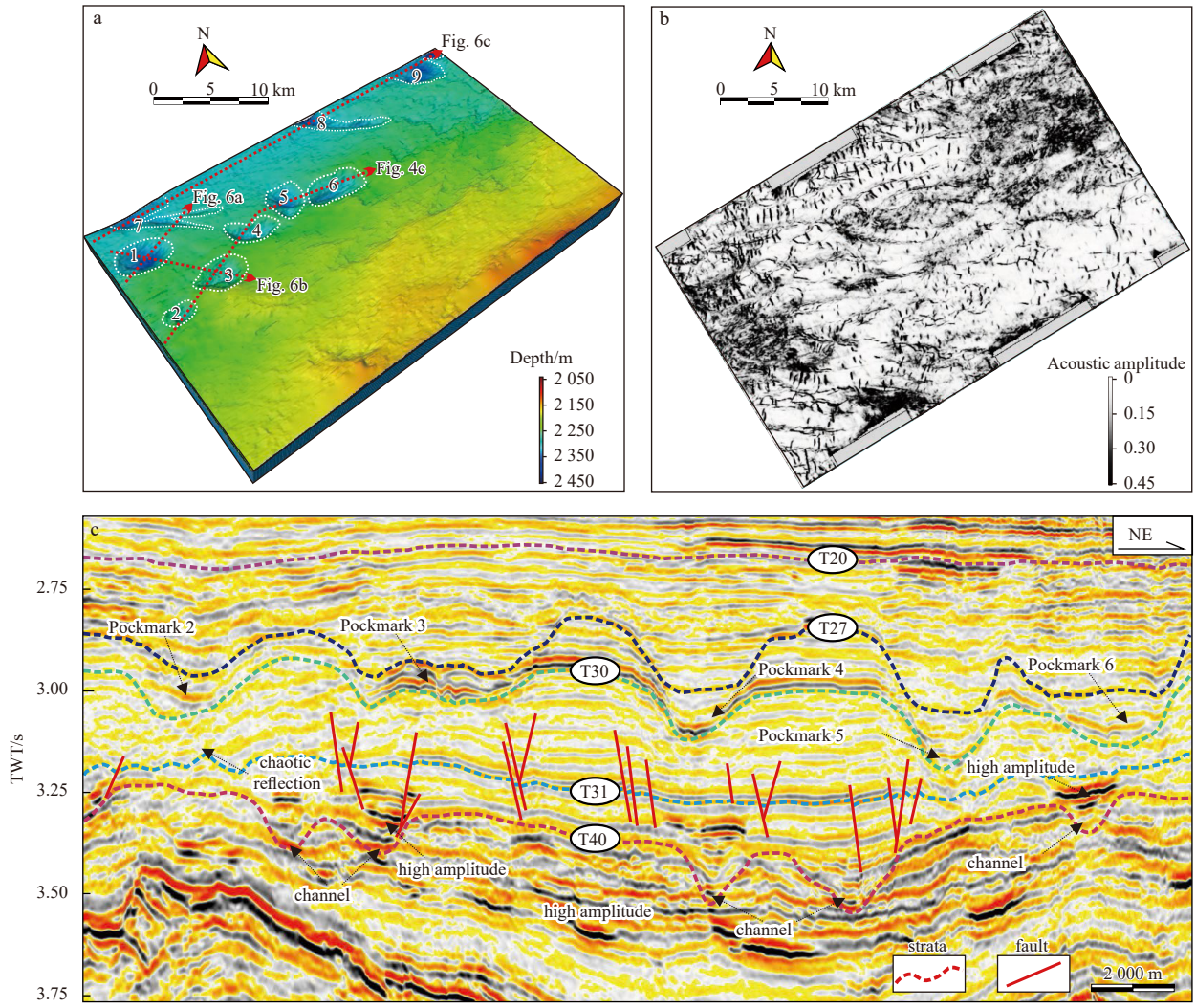

Fig. 4. Characteristics of the sedimentation period of the Yinggehai Formation in the study area: paleo-topographic map of Horizon T30 (a); coherence slice of Horizon T31 (b); and seismic reflection features (c).

Table 1. Summary of ancient pockmark characteristics in the study area

Number	Long axis/km	Short axis/km	Depth/km	Dip angle of the long axis/(°)	Trend	Profile shape	Planar shape
1	4.95	2.21	0.34	7.87	near NE	U	oval
2	2.29	1.25	0.43	21.52	near NE	U	oval
3	4.54	2.44	0.40	10.10	near NE	W	oval
4	4.18	1.56	0.36	9.87	near EW	U	crescent
5	2.75	1.68	0.60	25.00	near EW	U	oval
6	4.67	2.01	0.33	8.10	near NE	U	oval
7	12.04	10.66	1.03	9.80	near EW	V	chain
8	14.63	10.22	1.17	9.16	near EW	V	chain
9	9.16	7.38	1.25	15.64	near EW	W	oval

Note: The information provided for ancient Pockmarks 7, 8, and 9 comprises only the data collected within the research area, although these pockmarks extend past the study area.

or V-shaped (Fig. 7c). At the same time, obvious reflections of channel features can be identified, such as truncations (Fig. 7e).

5 Discussion

5.1 *Comparison of the characteristics of various geological bodies in the depression*

A pockmark is a typical depression landform (Sun et al., 2011; Pilcher and Argent, 2007; Böttner et al., 2019) that exhibits obvious stratum depression characteristics on seismic reflection (King and Maclean, 1970; Luo et al., 2012). In the studied section, channels and craters also exhibit obvious strata depression features (Fig. 8), but these landforms are essentially different from pockmarks.

5.1.1 *Submarine channels*

A submarine channel is a long strip of negative seafloor terrain formed under the actions of turbidity currents and related

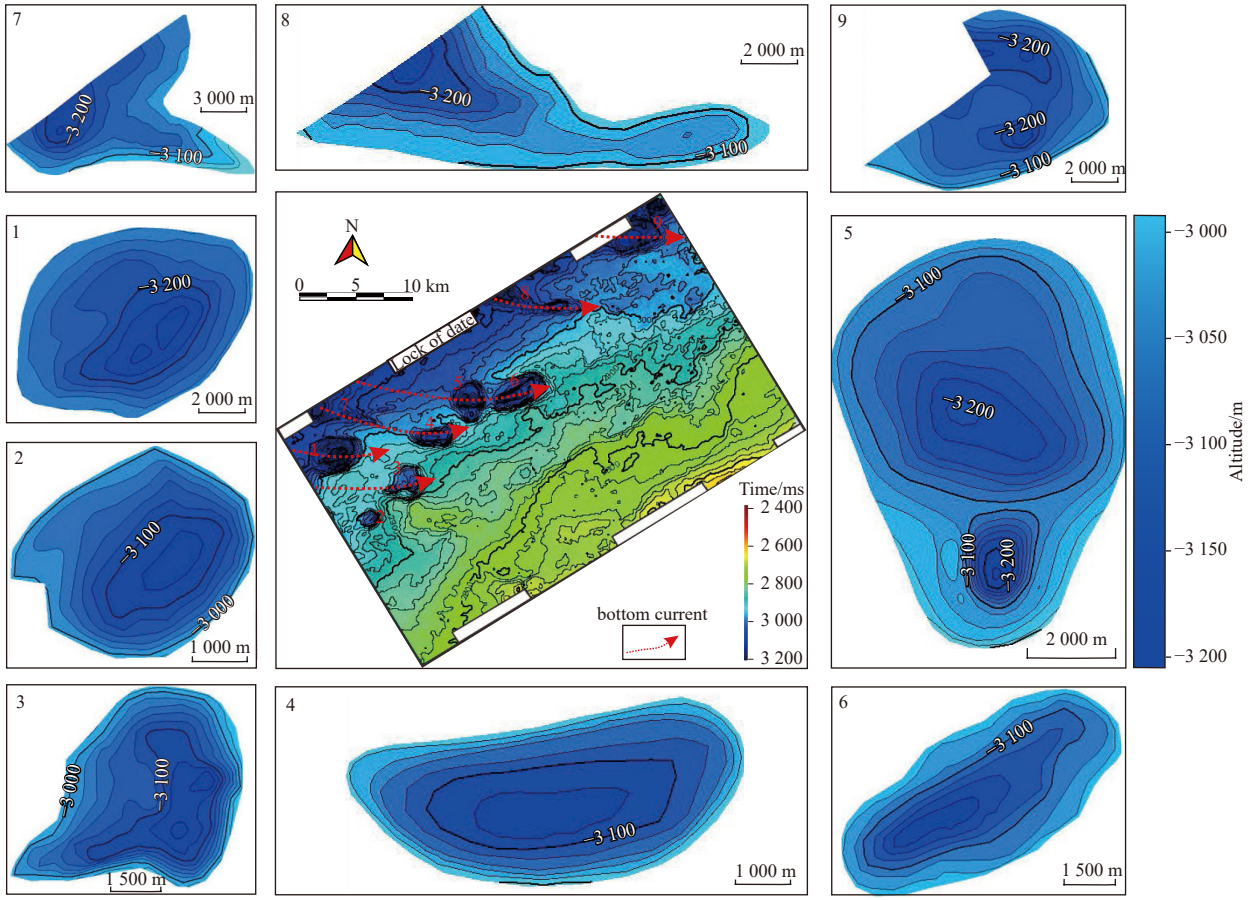

Fig. 5. Time structure diagram of the T30 Interface. Bottom current direction modified from Li et al. (2018c).

sedimentation processes; a submarine channel is the main passage by which sediments are transported to a basin (Tian et al., 2017). Due to the strong erosion effects experienced by the turbidite sediments on the underlying strata during this transportation process, relatively obvious erosion characteristics usually appear on the seismic-section strata in developed channels (Hassan et al., 2005). Therefore, truncation reflections can usually be observed on the seismic sections of channel development sites, embodying the characteristic reflection of a submarine channel (Tian et al., 2017; Selim, 2012). Because the deposition and filling of channel sands occur in the channel sedimentary body, these channels often show strong amplitudes in seismic sections (Sun et al., 2011; Li et al., 2018c; Tian et al., 2017). Channel deposition reflects a complete depositional process from the source to the sink and tends to exhibit good planar connectivity (Tian et al., 2017), while pockmarks usually develop at single points (Böttner et al., 2019). The paleogeomorphological analysis of the Yinggehai Formation in the study area revealed that several depressional structures are completely displayed in the area and are mutually independent (pockmark nos. 1–6). Although the geomorphological characteristics of depressions no. 7 and no. 8 reflect certain degrees of connectivity, the overall geomorphological characteristics of the study area indicate high terrain in the southeast and low terrain in the northwest during the depositional period of the Yinggehai Formation; therefore, the sediments did not reflect the conditions required to be transported and eroded from north to south through channels to form depressions no. 7 and no. 8. At the same time, judging from the geomorphological features of the depressions identified in the study area, multiple depression centers exist in the no. 3 and no. 9 depression structures but are not common in the channel sediments (Figs 4a and 6). In addition, no characteristic channel reflections, such as truncation reflections, were identified in the seismic sections of the Yinggehai Formation depressions in the study area (Figs 8d, e).

5.1.2 *Meteorite craters*

A crater is a concave landform formed when a meteorite hits a planet or moon; craters can be divided into simple and complex impact craters (Zhao et al., 2011). A simple crater is a single crater on the ground, usually no more than 4 km in diameter, while a complex crater is usually larger than a simple crater and exhibits a central peak, the result of the stratum being impacted and rebounding (Keerthy et al., 2019; Zhao et al., 2011). Meteorites exert strong impact forces, and obvious radial fissures tend to develop on crater walls, appearing as concentric annular faults on the plane; this is the most important structural feature of a crater (Keerthy et al., 2019; Wang et al., 2013) (Figs 8a, b). In a crater development area, typical shock-derived metamorphic features, such as molten rock, breccia lenses, and quartz shock surface lamination, can usually be identified (Keerthy et al., 2019; Zhao et al., 2011; Li et al., 2018a). Because the energy of a meteorite is concentrated on a soecufuc point on the surface of the Earth, most craters are circular, while a few form elongated shapes near the land surface when a meteorite is at an angle (Keerthy et al., 2019; Li et al., 2018a). No obvious annular fissures were observed in the seismic sections comprising the depression structures in the study area; in addition, the identified depression structures mostly appeared to exhibit crescent, ellipse, and

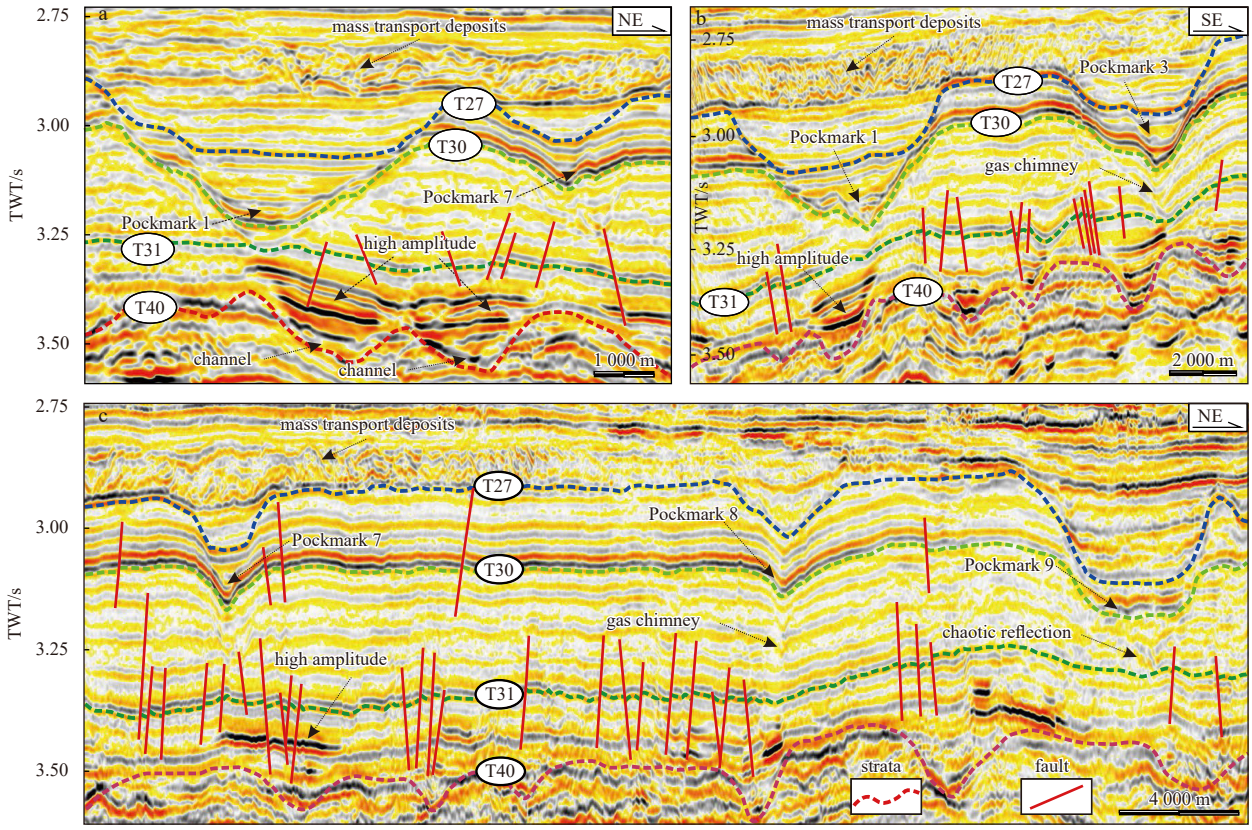

Fig. 6. Seismic reflection characteristics of the Yinggehai Formation depression landforms in the study area (section location shown in Fig. 4a).

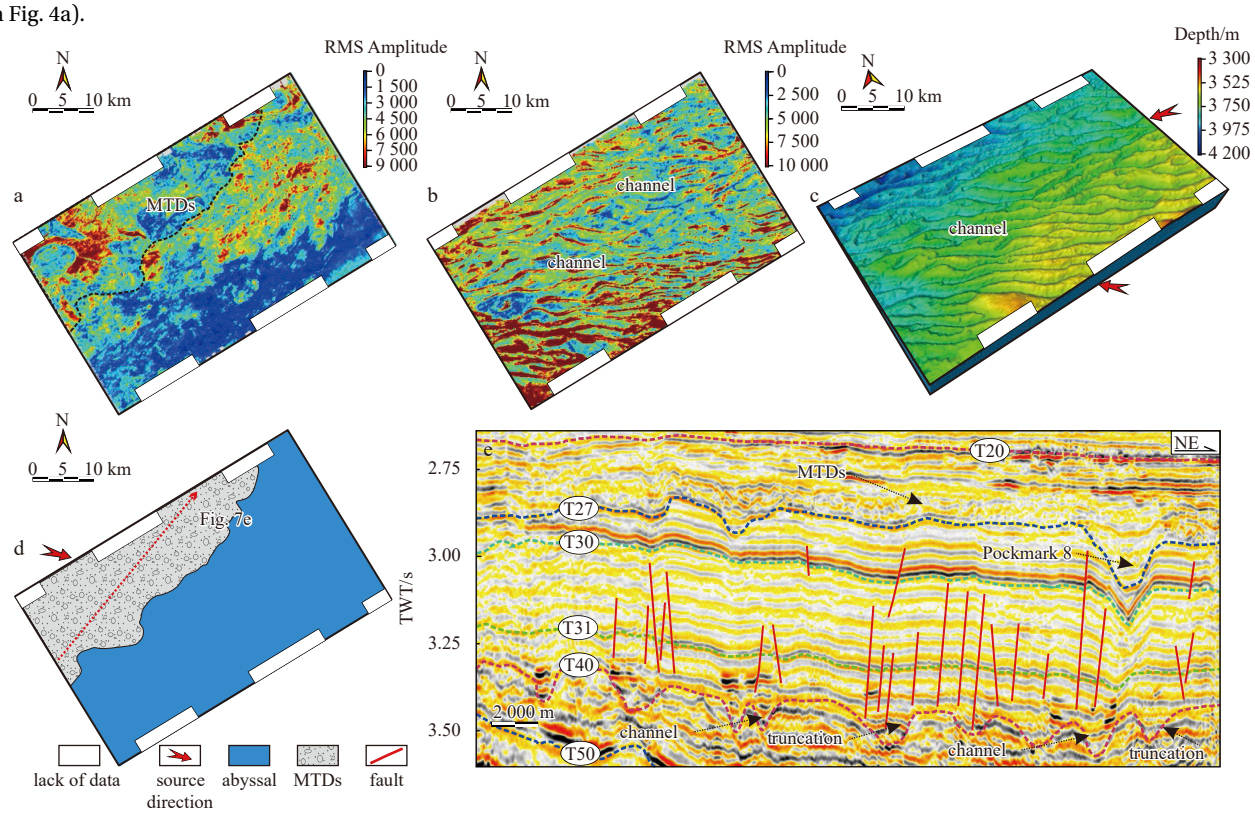

Fig. 7. Root mean square (RMS) amplitude map between Horizon T27 and 40 ms above Horizon T27 (a); RMS amplitude map between Horizon T40 and 40 ms above Horizon T40 (b); paleo-topographic map of Horizon T40 (c) (source direction from Xiong et al. (2021)); planar distributions of sedimentary systems between Horizons T27 and T20 (d) (source direction modified from Cheng et al. (2022)); characteristics of the Late Middle Miocene on the seismic profiles (e). See d for the location of e. MTDs: mass-transport deposits.

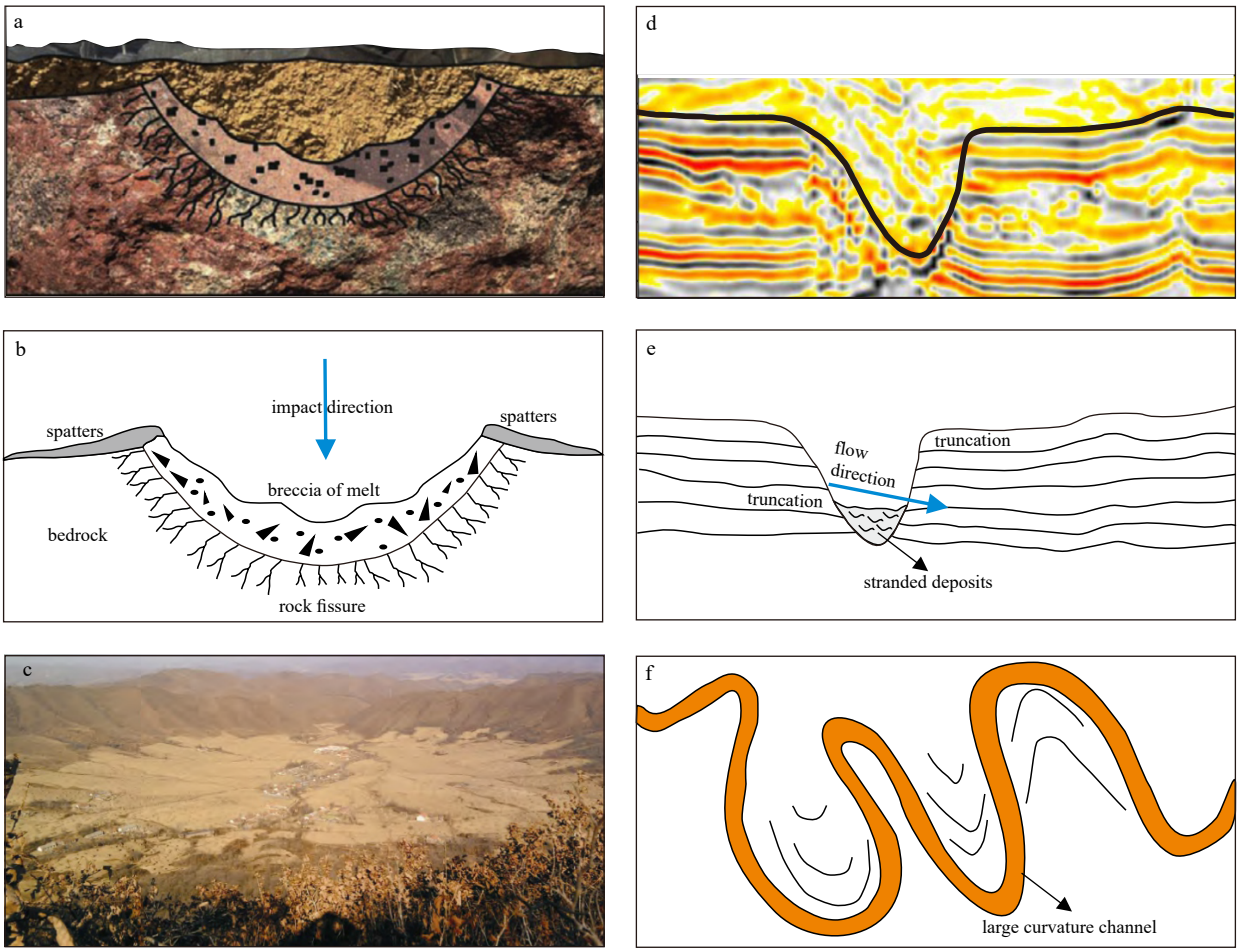

Fig. 8. Typical section structures of meteorite craters (a, b) (modified from Keerthy et al. (2019)); Xiuyan meteorite craters (c) (modified from Wang et al. (2013)); typical channel section structures (d, e) (modified from Tian et al. (2017)); and high-curvature channel deposits (f) (modified from Mayall et al. (2006)).

chain shapes, which differ significantly from the shapes of craters.

5.2 *Analysis of the genetic mechanism of the analyzed pockmarks*

A seabed pockmark is a depression landform that is formed by the fluid in the underlying strata escaping at a certain point on the seabed through a migration pathway and causing the seabed surface to collapse (Hovland and Sommerville, 1985; Hovland et al., 2002; Böttner et al., 2019). In this study, we found that the formation of the analyzed ancient pockmarks in the area included two stages: one involving the escape of deep fluid and one involving lateral reformation of the bottom current.

5.2.1 *Fluid escape system*

A fluid escape system mainly involves two aspects: “fluid” and “escape”. Fluid escape types include seepage escape and accumulated escape. Only when a fluid flows through a fault, gas chimney, or other special pathway resulting in accumulative escape is it possible to form pockmark landforms on the seabed (Sun et al., 2011). Of course, after the decomposition of natural gas hydrate in shallow seabed strata, there are often dents on the seabed, but the scale of such dents is usually limited. For example, the diameter of the pits formed by the submarine hydrate mound after the nucleation, uplift and extinction stages is generally 1–300 m (Hovland and Svensen, 2006).

Drilling activities have revealed multiple sets of source rocks in the Qiongdongnan Basin; for example, Miocene marine source rocks, Oligocene marine transitional source rocks and Eocene lacustrine source rocks, this basin has great potential for hydrocarbon generation at present (Lai et al., 2021; Fang et al., 2019; Cheng et al., 2021; Ren et al., 2022). In the deep strata, the Yacheng Formation has the best hydrocarbon generation potential and the highest organic matter abundance, which is a set of medium-good source rocks and is generally considered the main source rocks in the Qiongdongnan Basin. In particular, the coal measure source rocks in this set of strata have a wide distribution range and are a set of high-quality gas source rocks in the basin (Lai et al., 2021; Fang et al., 2019). Previous studies have confirmed that the Qiongdongnan Basin experienced multiple periods of overpressure conditions and pressure relief (Xie et al., 2016; Zhai et al., 2013). Since the depositional period of the Huangliu Formation in the Late Miocene, the source rocks located in the deep strata of the basin have gradually overmatured, and hydrocarbon cracking has enhanced (Zhai et al., 2013; Huang et al., 2016, 2017). The large-scale migration of natural gases to shallow formations has generally been seen in various sag formations (Zhai et al., 2013). In the depositional period of the Yinggehai Formation, the Qiongdongnan Basin already had a good hydrocarbon-generating capacity (Zhai et al., 2013; Huang et al., 2016, 2017). Judging from the developmental scale of the

ancient pockmarks in the study area, the fluid escape activity in the early Yinggehai Formation was likely relatively strong, indicating that the fluid escaped at a certain scale and that the fluid mainly originated from deep formations (Zhu et al., 2021). Obviously, pockmarks of this size in the study area are unlikely to be mainly formed by the decomposition of gas hydrates in shallow formations. However, it cannot be ruled out that gas hydrates were formed and decomposed in the shallow strata at that time and then participated in the formation process of the ancient pockmark.

Although the Qiongdongnan Basin has been stable overall since T60, hardly any large structural faults can be observed in the basin; however, local tectonic activity can be induced under superstrong pressure conditions, and stretched strata and small faults have developed and serve as optimal vertical fluid-migration pathways (Xie et al., 2016). On the other hand, large-scale sedimentary channel bodies developed during the depositional period of the Meishan Formation in the southern deep-water area of the Qiongdongnan Basin (Xiong et al., 2021). These channel sands are usually the predominant accumulation areas for fluids in the formation due to their relatively coarse sediment particle sizes (Xie et al., 2016). When the fluid in the channel sands continually accumulates to reach a certain scale, the overlying strata in the channel tend to develop compaction faults due to the high-pressure conditions, and these faults then provide migration pathways for fluids (Sun et al., 2011; Bai et al., 2014). Pockmarks have also been observed to develop above channel sediments on the current seafloor in the northern South China Sea (Zhu et al., 2021). During this process, channel sands played the role of accumulating fluids to facilitate the formation of overpressure conditions.

On the seismic profile of the study area, high-amplitude reflections due to gas accumulation and gas chimneys can be observed in the strata underlying the pockmarks, indicating that these underlying strata have optimal conditions for fluid accumulation (Figs 4c and 5). At the same time, in the Miocene Huangliu Formation, obvious interlayer small faults have also been observed; even between the Horizons of T31 and T20, there are interlayer faults that run through the T30 interface and terminates under the MTDs above the Horizon of T27 (Figs 4c and 5); similar faults have also been identified in other Miocene strata in the southern Qiongdongnan Basin (Li et al., 2018b; Sun et al., 2010). This indicates that the deep fluid leakage in the study area not only occurs in the floor layer under the pockmark but also continues for a period of time after the pockmark formation is formed, which is effectively blocked by the MTDs in the late Yinggehai Formation. It is clear that this continuous fluid leakage is much less severe due to the large amount of energy already released through the pockmark.

5.2.2 *Bottom-current erosion*

At the original formation stage, pockmarks are usually nearly circular in shape (Masoumi et al., 2014; Zhu et al., 2021; Yu et al., 2021) and are then often transformed by bottom currents or gravity currents until they finally take on a certain shape and scale (Luo et al., 2012; Bai et al., 2014; Yu et al., 2021). When a gravity current continuously acts on a pockmark landform, due to the strong erosional effect, a pockmark located in the flow direction is very likely to be transformed into a submarine channel (Yu et al., 2021). Although there is a trend of connectivity among the ancient pockmarks in the study area, the pockmarks are relatively independent overall and do not exhibit channel characteristics (Figs 4a and 5). In addition, from the perspective of ancient landforms, it would be difficult for gravitational currents to act in the study area to form the pockmark landforms observed in the area. Hence, bottom-current activity may be the main controlling factor determining the morphological changes observed in the ancient pockmarks in the study area. In addition to the influence of local topographic differences and other factors, the axes of elliptical, crescent-shaped and chain-shaped pockmarks often have good matching relationships with the bottom-current flow direction (Zhu et al., 2021; Dandapath et al., 2010), and the impact of the bottom current on the pockmark can even be greater than the effect of fluid escape (Sun et al., 2011).

Whether there is deep water in the Qiongdongnan Basin is still controversial, but some consensus has been reached with regard to the flow direction of the surface waters and middle waters in the basin (Tian et al., 2015; Chen et al., 2014, 2016; Gong et al., 2016). By studying the obvious erosion differences between the two sides of the seamounts near the Beijiao Sag in the Qiongdongnan Basin and by combining the results with the sedimentary characteristics and migration laws of the channel sedimentary bodies developed in the Miocene strata, Li et al. (2018c) reported that during the depositional period of the Miocene Huangliu Formation, a bottom current changed direction from EW to NE near the Beijiao Sag; this finding is consistent with previous judgments on the flow direction of the middle waters in the Qiongdongnan Basin (Palamenghi et al., 2015; Yang et al., 2008). Moreover, the Beijiao Sag has mainly been in a semideep-sea sedimentary environment since the depositional period of the Meishan Formation in the Miocene, and the middle waters play a major role in controlling the submarine sediments (Li et al., 2018c). Under the condition that the tectonic setting of the basin tends to be stable, the direction of the middle waters usually does not change extensively (Li et al., 2018c; Palamenghi et al., 2015); that is, the bottom-current activity oriented in this direction near the Beijiao Sag continued at least until the deposition of the Yinggehai Formation.

The trends of the ancient pockmarks in the study area mainly include the east–west direction, and the southeast sides of the insides of the ancient pockmarks are steeper than the other pockmark surfaces (Figs 4a, 5 and 6b), indicating that the bottom current eroded the ancient pockmarks from west to east; the paleo-bottom current in the study area in the Miocene was likely oriented in the east–west direction (Yu et al., 2021; Bai et al., 2014; Sun et al., 2011). Except for bottom-current erosion, the ancient landforms in the study area, which were high in the south and east and low in the north and west, also impacted the shape of the pockmarks, thus resulting in the pockmarks in the study area trending nearly northeast. Therefore, during the depositional period of the Yinggehai Formation, the bottom current near the Beijiao Sag in the southern region of the Qiongdongnan Basin was oriented nearly east–west, while slight differences arose in local areas due to geomorphological conditions and other factors (Fig. 5). This finding is consistent with the results of previous studies on the flow direction of the paleo-bottom current in the deep-water area in the southern region of the Qiongdongnan Basin (Li et al., 2018c; Palamenghi et al., 2015).

5.3 *Evolution process of giant ancient pockmarks*

According to our analyses of the seismic reflection, fluid escape, and bottom current transformation characteristics of the giant pockmarks in the Yinggehai Formation in the southern part of the Qiongdongnan Basin, these pockmarks have undergone the following evolution pattern: since the sedimentary period of the Miocene Huangliu Formation, the deep hydrocarbon source

rocks in the Qiongdongnan Basin have gradually become overmature, and the overpressure formed by hydrocarbon hydrolysis has caused the development of small faults. Driven by strong formation pressure, deep fluids, which are hydrocarbon-rich fluids and composed of formation water, deep stratum material and hydrocarbons, have gradually migrated to shallow formations through advantageous paths such as faults and gas chimneys to release energy. Passing through the Meishan Formation, these deep fluids tend to accumulate in the channel sands of the Meishan Formation (Fig. 9a). When the fluids in the channel sands of the Meishan Formation reach a certain scale, they preferentially release energy to the weak areas in the overlying strata to form small faults or gas chimneys and then accumulate and escape through those pathways. Thus, leakage occurred in the ancient seabed in the early depositional stage of the Yinggehai Formation to form nearly circular pockmarks, the most primitive form of a pockmark (Fig. 9b). After the formation of the original ancient pockmarks, the pockmarks were eroded and transformed by the near-E–W-trending paleo-bottom current in the southern region of the Qiongdongnan Basin (Fig. 9c), and the initially nearly circular ancient pockmarks were gradually transformed to exhibit near-E–W trends. Due to local topographic differences, oval-, crescent- and chain-shaped ancient pockmarks formed, and the closely spaced pockmarks were connected on the plane due to the transformational effect of the bottom current, thus forming chain-shaped ancient pockmarks. Then, the effective caprock deposited in the late depositional period of the overlying Yinggehai Formation prevented the development of pockmarks in multiple subsequent stages (Fig. 9).

5.4 *Impact on paleoclimate*

A pockmark is a characteristic landform that forms when deep-formation fluid leaks onto the seabed. The process by which deep-formation fluid migrates upward involves three stages: (1) reaction with sediments; (2) breaking through the sediments and reacting with seawater; and (3) breaking through the hydrosphere and entering the atmosphere (Lai, 2007; Dickens, 2003; Katz et al., 1999).

Hydrocarbons and sulfate minerals in seafloor sediments undergo anaerobic oxidation in anoxic environments, including the anaerobic oxidation of methane, resulting in carbonate precipitation and carbon dioxide; these substances can then provide sufficient carbon sources and energy for biological processes (Fig. 10a), ultimately promoting the development of biomes, such as the Cold Springs biome (Katz et al., 1999; Dickens, 2003). The efficiency with which hydrocarbons are consumed in sediments is related to various factors, such as the fluid velocity, seafloor topography, and bottom current activities (Lai, 2007). When hydrocarbons cannot be completely consumed by sediments, they break through the sediments and enter the hydrosphere (Fig. 10).

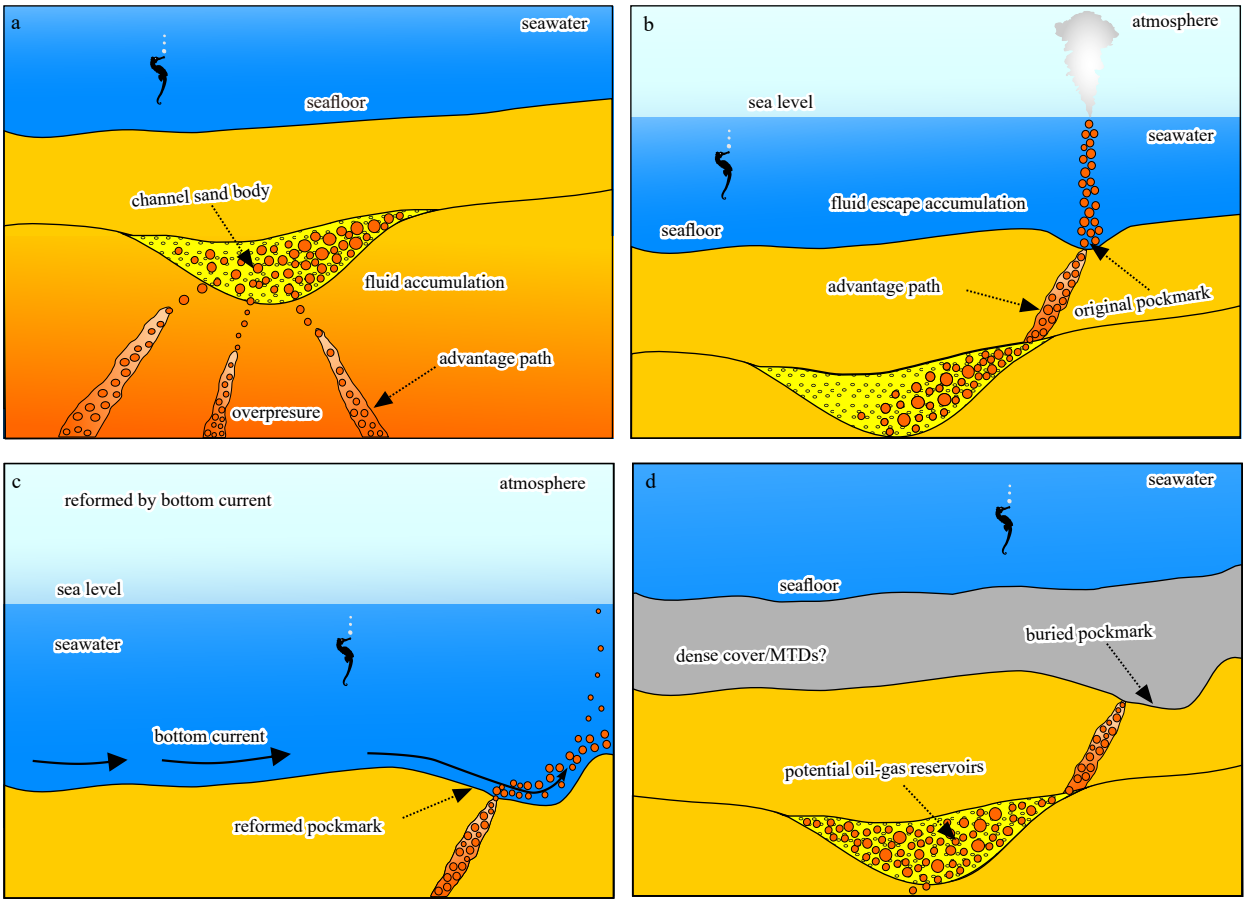

Fig. 9. The evolution model of the giant ancient pockmarks in the Qiongdongnan Basin. Overpressure built up, and deep fluids accumulated in the channel sands (a); the fluid in the channel sands escaped following accumulation, forming near-circular ancient pockmarks on the seafloor (b); affected by bottom-current erosion, these ancient pockmarks were transformed into different shapes (c); and the overlying effective capping prevented the ancient pockmarks from developing in multiple stages, causing the pockmarks to be buried in the stratum (d).

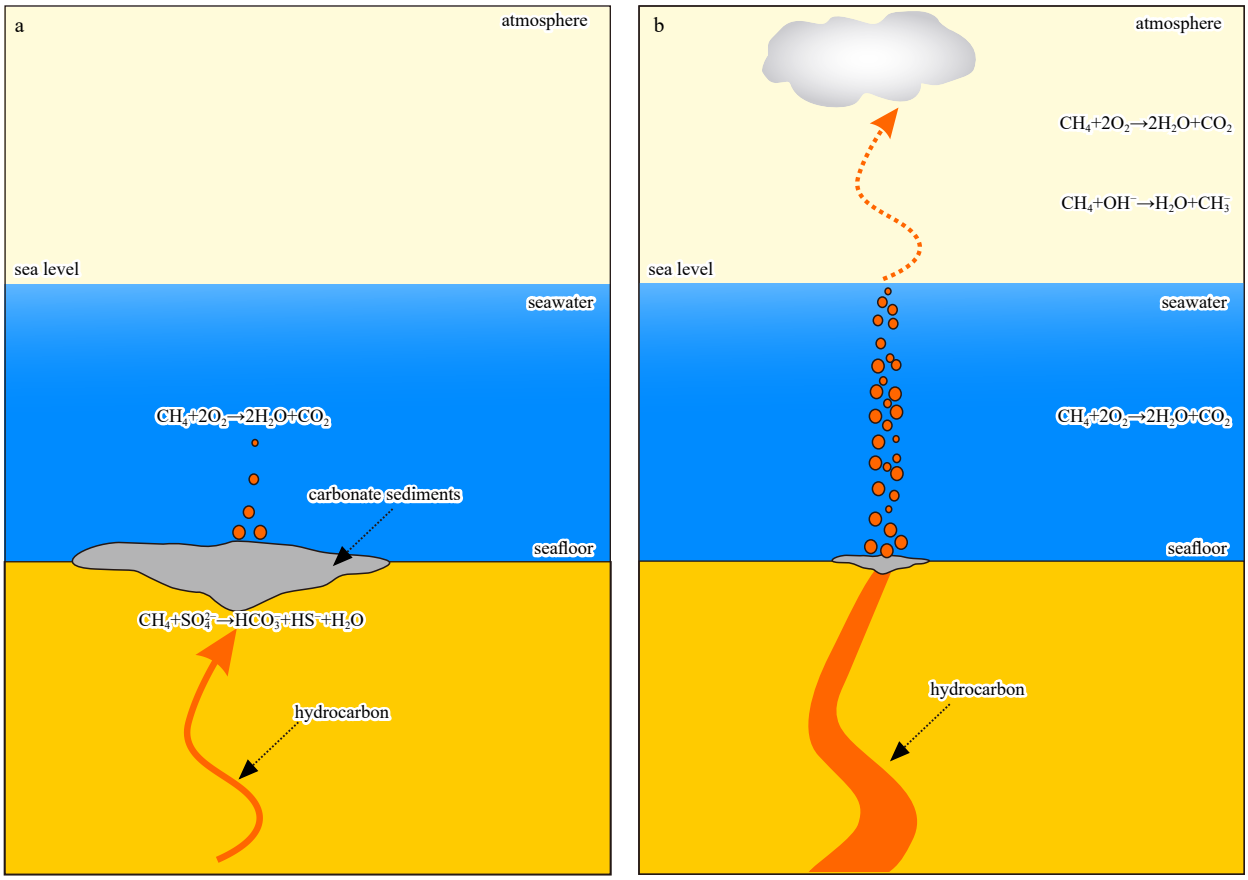

Fig. 10. Slight leakage of deep-formation fluids, most of which reacted with seabed sediments to form carbonate precipitation, while a few reacted with seawater and failed to break through the hydrosphere (a); intense deep-formation fluid leakage, most of which broke through the hydrosphere and entered the atmosphere, while a small part reacted with the seawater and seafloor sediments (b) (redrawn after Katz et al. (1999) and Dickens (2003)).

At this stage, factors such as solubility, oxidation, and upwelling in the seawater play leading roles in the consumption of hydrocarbons in seawater (Dickens, 2003). The oxidation and dissolution of seawater cause hydrocarbons to be consumed. If the oxygen content of seawater is high, hydrocarbons can be consumed in large quantities. For example, more than 80% of the methane in submarine thermogenic gases can be consumed in this process (Dickens, 2003; Lai, 2007). This upwelling activity helps hydrocarbons pass through the hydrosphere and enter the atmosphere (Dickens, 2003). Generally, only a small amount of hydrocarbons can enter the atmosphere after reacting with sediments and seawater. However, when deep fluids are released violently on the seafloor, such as in mud volcanoes and pockmarks, hydrocarbons can quickly break through the sediments, enter the hydrosphere, and rise rapidly (Judd et al., 2002). In this process, sediments and seawater have little effect on the fluids, and most hydrocarbons can enter the atmosphere and then impact the environmental climate; this process has been confirmed in studies of short-term global warming in the Quaternary (Brook et al., 1996). The giant pockmarks in the study area indicate that deep fluid was active during this period, as can be observed in the seismic sections obtained for many areas in the Qiongdongnan Basin. This finding shows that most of the hydrocarbons present in the deep fluids at that time could break through the sediments and hydrosphere, enter the atmosphere quickly, and then impact the paleoclimate (Fig. 10b).

The application of isotopes has enabled the reconstruction of paleoclimatic information. Previous studies have shown that the overall atmospheric CO_2 concentration in the global low latitudes exhibits an upward trend at approximately 6.5–5.5 Ma, while after 5.5 Ma, the atmospheric CO_2 concentration began to decline (Fig. 11). This finding corresponds to the Qiongdongnan Basin releasing greenhouse gases into the atmosphere through giant ancient pockmarks during the early deposition of the Yinggehai Formation, while the caprock that formed during the late deposition of the Yinggehai Formation effectively prevented deep fluids from continuing to release greenhouse gases into the

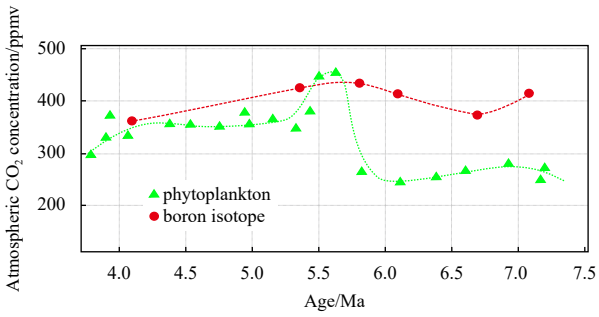

Fig. 11. Reconstructed records of atmospheric CO_2 concentrations from different metrics ranging from 7.5 Ma to 4.0 Ma (redrawn after Wei and Tian (2022); dates are referenced from Sosdian et al. (2018) and Breecker and Retallack. (2014)).

atmosphere. In addition, multiple wells, such as LS33-1-1 and YL19-1-1, revealed an order of magnitude decrease in the abundance of planktic foraminifera, which represents high productivity, in the Qiongdongnan Basin during the late Miocene (Li, 2013; Li et al., 2021). This is partly related to the large leakage of deep hydrocarbon-rich fluids through the pockmark, which affects the marine environment.

6 Conclusions

The characteristics and nature of the giant ancient pockmarks in the Qiongdongnan Basin were illustrated in this study using 2D and high-precision 3D seismic data. In addition, the genetic mechanism of the ancient pockmarks in the study area, their impacts on the paleoenvironment were also discussed. The main conclusions are described as follows:

(1) Giant ancient pockmarks are present in the Yinggehai Formation of the Qiongdongnan Basin. The longest diameter among these ancient pockmarks is 4.95 km, the shortest long-axis diameter is 2.29 km, and the maximum depth is 0.33 km. The overall trend of the ancient pockmarks is nearly E–W, and the pockmarks are oval-, crescent- and chain-shaped on the plane and U-, V- and W-shaped on the seismic profile.

(2) The giant ancient pockmarks of the Yinggehai Formation in the Qiongdongnan Basin were formed under the common influence of the escape of deeply accumulated fluid and lateral transformation of the bottom current. The overpressure formed by the thermal evolution of the deep source rocks in the basin provided the impetus for the upward migration of fluids. This upward migration caused deep fluid to tend to accumulate in favorable accumulation areas, causing the formation pressure in these fluid accumulation areas to continuously increase. With time, interlayer faults or gas chimneys formed in the weak area of overlying strata, and the accumulated fluid escaped from these pathways, forming nearly circular ancient pockmarks on the ancient seabed. Afterward, due to the erosion and transformation of the near-EW bottom current, the ancient pockmarks evolved into different shapes. Finally, the overlying dense and effective caprock prevented ancient pockmarks from developing in the strata throughout multiple stages.

(3) Pockmarks are a sign of intensive deep-fluid escape. Fluids escaping through pockmarks are likely to break through the hydrosphere and enter the atmosphere, where they impact the atmospheric environment. At approximately 6.5–5.5 Ma, a large amount of greenhouse gas was released from the Qiongdongnan Basin into the atmosphere through the giant ancient pockmarks, thus causing significant increases in atmospheric CO_2 and other gases. Later, affected by the overlying effective cover, the ancient pockmarks stopped developing, thus slowing down the large-scale release of greenhouse gases into the atmosphere and reducing the concentrations of CO_2 and other greenhouse gases in the atmosphere.

Acknowledgements

We would like to thank the Guangzhou Marine Geological Survey (http://www.gmgs.cgs.gov.cn/) for providing the seismic data used in this study, as these data provided us great support. Thanks also go to the reviewers and editors for their contributions to improving this paper.

References

Bai Yang, Song Haibin, Guan Yongxian, et al. 2014. Structural characteristics and genesis of pockmarks in the northwest of the South China Sea derived from reflective seismic and multibeam data. Chinese Journal of Geophysics (in Chinese), 57(7): 2208–2222

Böttner C, Berndt C, Reinardy B T I, et al. 2019. Pockmarks in the Witch Ground Basin, Central North Sea. Geochemistry, Geophysics, Geosystems, 20(4): 1698–1719, doi: 10.1029/2018GC008068

Breecker D O, Retallack G J. 2014. Refining the pedogenic carbonate atmospheric CO_2 proxy and application to Miocene CO_2. Palaeogeography, Palaeoclimatology, Palaeoecology, 406: 1–8, doi: 10.1016/j.palaeo.2014.04.012

Brook E J, Sowers J, Orchardo J. 1996. Rapid variations in atmospheric methane concentration during the past 110, 000 years. Science, 273(5278): 1087–1091, doi: 10.1126/science.273.5278.1087

Cao Licheng, Jiang Tao, Wang Zhenfeng, et al. 2015. Provenance of Upper Miocene sediments in the Yinggehai and Qiongdongnan basins, northwestern South China Sea: Evidence from REE, heavy minerals and zircon U–Pb ages. Marine Geology, 361: 136–146, doi: 10.1016/j.margeo.2015.01.007

Chen Jiangxin, Song Haibin, Guan Yongxian, et al. 2015. Morphologies, classification and genesis of pockmarks, mud volcanoes and associated fluid escape features in the northern Zhongjiannan Basin, South China Sea. Deep-Sea Research Part II: Topical Studies in Oceanography, 122: 106–117, doi: 10.1016/j.dsr2.2015.11.007

Chen Jiangxin, Song Haibin, Guan Yongxian, et al. 2018. Geological and oceanographic controls on seabed fluid escape structures in the northern Zhongjiannan Basin, South China Sea. Journal of Asian Earth Sciences, 168: 38–47, doi: 10.1016/j.jseaes.2018.04.027

Chen Hui, Xie Xinong, Van Rooij D, et al. 2014. Depositional characteristics and processes of alongslope currents related to a seamount on the northwestern margin of the Northwest Sub-Basin, South China Sea. Marine Geology, 355: 36–53, doi: 10.1016/j.margeo.2014.05.008

Chen Hui, Xie Xinong, Zhang Wenyan, et al. 2016. Deep-water sedimentary systems and their relationship with bottom currents at the intersection of Xisha Trough and Northwest Sub-Basin, South China Sea. Marine Geology, 378: 101–113, doi: 10.1016/j.margeo.2015.11.002

Cheng Cong, Jiang Tao, Kuang Zenggui, et al. 2021. Seismic characteristics and distributions of Quaternary mass transport deposits in the Qiongdongnan Basin, northern South China Sea. Marine and Petroleum Geology, 129: 105118, doi: 10.1016/j.marpetgeo.2021.105118

Cheng Cong, Kuang Zenggui, Jiang Tao, et al. 2022. Source of the sand-rich gas hydrate reservoir in the northern South China Sea: Insights from detrital zircon U–Pb geochronology and seismic geomorphology. Marine and Petroleum Geology, 145: 105904, doi: 10.1016/j.marpetgeo.2022.105904

Dandapath S, Chakraborty B, Karisiddaiah S M, et al. 2010. Morphology of pockmarks along the western continental margin of India: Employing multibeam bathymetry and backscatter data. Marine and Petroleum Geology, 27(10): 2107–2117, doi: 10.1016/j.marpetgeo.2010.09.005

Davy B, Pecher I, Wood R, et al. 2010. Gas escape features off New Zealand: Evidence of massive release of methane from hydrates. Geophysical Research Letters, 37(21): L21309, doi: 10.1029/2010GL045184

Dickens G R. 2003. Rethinking the global carbon cycle with a large, dynamic and microbially mediated gas hydrate capacitor. Earth and Planetary Science Letters, 213(3–4): 169–183, doi: 10.1016/S0012-821X(03)00325-X

Fang Yunxin, Wei Jianggong, Lu Hailong, et al. 2019. Chemical and structural characteristics of gas hydrates from the Haima cold seeps in the Qiongdongnan Basin of the South China Sea. Journal of Asian Earth Sciences, 182: 103924, doi: 10.1016/j.jseaes.2019.103924

Geng Minghui, Song Haibin, Guan Yongxian, et al. 2017. Characteristics and generation mechanism of gullies and mega-pockmarks in the Zhongjiannan Basin, western South China Sea. Interpretation, 5(3): SM49–SM59, doi: 10.1190/INT-2016-0216.1

Gong Chenglin, Wang Yingmin, Zheng Rongcai, et al. 2016. Middle

Miocene reworked turbidites in the Baiyun Sag of the Pearl River Mouth Basin, northern South China Sea margin: Processes, genesis, and implications. Journal of Asian Earth Sciences, 128: 116–129, doi: 10.1016/j.jseaes.2016.06.025

Guan Yongxian, Luo Min, Chen Linying, et al. 2014. Tracing study on the activity of mega-pockmarks in southwestern Xisha Uplift, South China Sea. Geochimica, 43(6): 628–639, doi: 10.19700/j.0379-1726.2014.06.007

Haq B U, Hardenbol J, Vail P R. 1987. Chronology of fluctuating sea levels since the Triassic. Science, 235(4793): 1156–1167, doi: 10.1126/science.235.4793.1156

Hassan M A, Church M, Lisle T E, et al. 2005. Sediment transport and channel morphology of small, forested streams. Journal of the American Water Resources Association, 41(4): 853–876, doi: 10.1111/j.1752-1688.2005.tb03774.x

Hovland M, Gardner J V, Judd A G. 2002. The significance of pockmarks to understanding fluid flow processes and geohazards. Geofluids, 2(2): 127–136, doi: 10.1046/j.1468-8123.2002.00028.x

Hovland M, Sommerville J H. 1985. Characteristics of two natural gas seepages in the North Sea. Marine and Petroleum Geology, 2(4): 319–326, doi: 10.1016/0264-8172(85)90027-3

Hovland M, Svensen H. 2006. Submarine pingoes: Indicators of shallow gas hydrates in a pockmark at Nyegga, Norwegian Sea. Marine Geology, 228(1–4): 15–23, doi: 10.1016/J.MARGEO.2005.12.005

Huang Heting, Huang Baojia, Huang Yiwen, et al. 2017. Condensate origin and hydrocarbon accumulation mechanism of the deepwater giant gas field in western South China Sea: A case study of Lingshui 17–2 gas field in Qiongdongnan Basin. Petroleum Exploration and Development, 44(3): 409–417, doi: 10.1016/S1876-3804(17)30047-2

Huang Baojia, Tian Hui, Li Xushen, et al. 2016. Geochemistry, origin and accumulation of natural gases in the deepwater area of the Qiongdongnan Basin, South China Sea. Marine and Petroleum Geology, 72: 254–267, doi: 10.1016/j.marpetgeo.2016.02.007

Jiang Tao, Xie Xinong, Wang Zhenfeng, et al. 2013. Seismic features and origin of sediment waves in the Qiongdongnan Basin, northern South China Sea. Marine Geophysical Research, 34(3–4): 281–294, doi: 10.1007/s11001-013-9198-0

Judd A, Hovland M. 2007. Seabed Fluid Flow: The Impact on Geology, Biology and the Marine Environment. Cambridge: Cambridge University Press, 408–409

Judd A G, Hovland M, Dimitrov L I, et al. 2002. The geological methane budget at Continental Margins and its influence on climate change. Geofluids, 2(2): 109–126, doi: 10.1046/j.1468-8123.2002.00027.x

Katz M E, Pak D K, Dickens G R, et al. 1999. The source and fate of massive carbon input during the Latest Paleocene thermal maximum. Science, 286(5444): 1531–1533, doi: 10.1126/science.286.5444.1531

Keerthy S, Vishnu C L, Li Shanshan, et al. 2019. Reconstructing the dimension of Dhala Impact Crater, Central India, through integrated geographic information system and geological records. Planetary and Space Science, 177: 104691, doi: 10.1016/j.pss.2019.07.006

King L H, Maclean B. 1970. Pockmarks on the Scotian Shelf. GSA Bulletin, 81(10): 3141–3148, doi: 10.1130/0016-7606(1970)81[3141:Potss]2.0.Co;2

Lai C C A. 2007. Effects of gas hydrates on the chemical and physical properties of seawater. Journal of Petroleum Science & Engineering, 56(1–3): 47–53, doi: 10.1016/j.petrol.2006.03.030

Lai Hongfei, Fang Yunxin, Kuang Zenggui, et al. 2021. Geochemistry, origin and accumulation of natural gas hydrates in the Qiongdongnan Basin, South China Sea: Implications from site GMGS5-W08. Marine and Petroleum Geology, 123: 104774, doi: 10.1016/j.marpetgeo.2020.104774

Lei Chao, Ren Jianye. 2016. Hyper-extended rift systems in the Xisha Trough, northwestern South China Sea: Implications for extreme crustal thinning ahead of a propagating ocean. Marine and Petroleum Geology, 77(33): 846–864, doi: 10.1016/j.marpetgeo.2016.07.022

Li Qianyu. 2009. The South China Sea: Paleoceanography and Sedimentology. Dordrecht: Springer Netherlands, 75–170, doi: 10.1007/978-1-4020-9745-4_3

Li Na. 2013. The sedimentary paleoenvironment and provenance analysis in deepwater area of Qiongdongnan Basin since Oligocene (in Chinese)[dissertation]. Qingdao: Ocean University of China, doi: 10.7666/d.D326675

Li Shanshan, Keerthy S, Santosh M, et al. 2018a. Anatomy of impactites and shocked zircon grains from Dhala reveals Paleoproterozoic meteorite impact in the Archean basement rocks of Central India. Gondwana Research, 54: 81–101, doi: 10.1016/j.gr.2017.10.006

Li Yufeng, Pu Renhai, Qu Hongjun, et al. 2018b. Distribution of bottom current channels and mounds controlled by Paleo-Morphology in Mid-Miocene in Beijiao Sag of Qiongdongnan Basin. Geological Science and Technology Information (in Chinese), 37(2): 1–8, doi: 10.19509/j.cnki.dzkq.2018.0201

Li Yufeng, Pu Renhai, Zhang Gongcheng. 2018c. Direction and deposition/erosion characteristics of the bottom currents in the QDNB, northwestern South China Sea. Progress in Geophysics (in Chinese), 33(6): 2546–2554, doi: 10.6038/pg2018BB0567

Li Yufeng, Pu Renhai, Zhang Gongcheng, et al. 2021. Characteristics and origins of ridges and troughs on the top of the middle Miocene strata in the Beijiao Sag of the Qiongdongnan Basin, northern South China Sea. Interpretation, 9(2): SB1–SB15, doi: 10.1190/INT-2020-0109.1

Liang Jinqiang, Fu Shaoying, Chen Fang, et al. 2017. Characteristics of methane seepage and gas hydrate reservoir in the northeastern slope of South China Sea. Natural Gas Geoscience (in Chinese), 28(5): 761–770, doi: 10.11764/j.issn.1672-1926.2017.02.006

Lin Meihua. 1995. Submarine geomorphology of the eastern continental shelf of the Hainan Island. Marine Geology and Quaternary Geology (in Chinese), 4(4): 37–46, doi: 10.16562/j.cnki.0256-1492.1995.04.004

Liu Xingjian, Tang Dehao, Yan Pin, et al. 2017. Characteristics of authigenic carbonates from a mega-pockmark on the eastern side of Baiyun Sag, South China Sea and their geological significance. Marine Geology and Quaternary Geology (in Chinese), 37(6): 119–127, doi: 10.16562/j.cnki.0256-1492.2017.06.013

Lu Yintao, Luan Xiwu, Lu Fuliang, et al. 2017. Seismic evidence and formation mechanism of gas hydrates in the Zhongjiannan Basin, western margin of the South China Sea. Marine and Petroleum Geology, 84: 274–288, doi: 10.1016/j.marpetgeo.2017.04.005

Luo Min, Wu Lushan, Chen Duofu. 2012. Research status and progress of seabed pockmarks. Marine Geology Frontiers (in Chinese), 28(5): 33–42, doi: 10.16028/j.1009-2722.2012.05.009

Masoumi S, Reuning L, Back S, et al. 2014. Buried pockmarks on the Top Chalk surface of the Danish North Sea and their potential significance for interpreting palaeocirculation patterns. International Journal of Earth Sciences, 103(2): 563–578, doi: 10.1007/s00531-013-0977-2

Mayall M, Jones E, Casey M. 2006. Turbidite channel reservoirs—Key elements in facies prediction and effective development. Marine and Petroleum Geology, 23(8): 821–841, doi: 10.1016/j.marpetgeo.2006.08.001

Palamenghi L, Keil H, Spiess V. 2015. Sequence stratigraphic framework of a mixed turbidite-contourite depositional system along the NW slope of the South China Sea. Geo-Marine Letters, 35(1): 1–21, doi: 10.1007/s00367-014-0385-z

Pilcher R, Argent J. 2007. Mega-pockmarks and linear pockmark trains on the West African continental margin. Marine Geology, 244(1–4): 15–32, doi: 10.1016/j.margeo.2007.05.002

Ren Jinfeng, Cheng Cong, Xiong Pengfei, et al. 2022. Sand-rich gas hydrate and shallow gas systems in the Qiongdongnan Basin, northern South China Sea. Journal of Petroleum Science and Engineering, 215: 110630, doi: 10.1016/j.petrol.2022.110630

Ren Jianye, Lei Chao. 2011. Tectonic stratigraphic framework of Yinggehai-Qiongdongnan Basins and its implication for tectonic province division in South China Sea. Chinese Journal of

Geophysics (in Chinese), 54(12): 3303–3314, doi: 10.3969/j.issn.0001-5733.2011.12.028

Selim E S I. 2012. The use of seismic interpretation for delineating the characteristic features of Messinian channels in the north Nile Delta, Egypt. Arabian Journal of Geosciences, 5(4): 713–722, doi: 10.1007/s12517-010-0248-5

Sosdian S M, Greenop R, Hain M P, et al. 2018. Constraining the evolution of Neogene ocean carbonate chemistry using the boron isotope pH proxy. Earth and Planetary Science Letters, 498: 362–376, doi: 10.1016/j.epsl.2018.06.017

Su Ming, Li Junliang, Jiang Tao, et al. 2009. Morphological features and formation mechanism of Central Canyon in the Qiongdongnan Basin, northern South China Sea. Marine Geology and Quaternary Geology (in Chinese), 29(4): 85–93, doi: 10.3724/sp.J.1140.2009.04085

Sun Qiliang, Cartwright J, Lüdmann T, et al. 2017. Three-dimensional seismic characterization of a complex sediment drift in the South China Sea: Evidence for unsteady flow regime. Sedimentology, 64(3): 832–853, doi: 10.1111/sed.12330

Sun Zhen, Wang Zhenfeng, Sun Zhipeng, et al. 2015. Structure and kinematic analysis of the deepwater area of the Qiongdongnan Basin through a seismic interpretation and analogue modeling experiments. Acta Oceanologica Sinica, 34(4): 32–40, doi: 10.1007/s13131-015-0585-z

Sun Qiliang, Wu Shiguo, Hovland M, et al. 2011. The morphologies and genesis of mega-pockmarks near the Xisha Uplift, South China Sea. Marine and Petroleum Geology, 28(6): 1146–1156, doi: 10.1016/j.marpetgeo.2011.03.003

Sun Qiliang, Wu Shiguo, Lü Fuliang, et al. 2010. Polygonal faults and their implications for hydrocarbon reservoirs in the southern Qiongdongnan Basin, South China Sea. Journal of Asian Earth Sciences, 39(5): 470–479, doi: 10.1016/j.jseaes.2010.04.002

Sun Tiantian, Wu Daidai, Pan Mengdi, et al. 2018. Geochemical characteristics of surface sediments in the southern Qiongdongnan Basin of the northern South China Sea and its implication for sedimentary environment. Journal of Tropical Oceanography (in Chinese), 37(4): 70–80, doi: 10.11978/2017091

Tian Dongmei, Jiang Tao, Zhang Daojun, et al. 2017. Genesis mechanism and characteristics of submarine channel: A case study of the first member of Yinggehai Formation in Ledong area of Yinggehai Basin. Earth Science (in Chinese), 42(1): 130–141, doi: 10.3799/dqkx.2017.010

Tian Jie, Wu Shiguo, Lv Fuliang, et al. 2015. Middle Miocene mound-shaped sediment packages on the slope of the Xisha carbonate platforms, South China Sea: Combined result of gravity flow and bottom current. Deep-Sea Research Part II: Topical Studies in Oceanography, 122: 172–184, doi: 10.1016/j.dsr2.2015.06.016

Tozer B, Sandwell D T, Smith W H F, et al. 2019. Global bathymetry and topography at 15 arc sec: SRTM15+. Earth and Space Science, 6(10): 1847–1864, doi: 10.1029/2019EA000658

Wang Xinyuan, Luo Lei, Guo Huadong, et al. 2013. Cratering process and morphological features of the Xiuyan impact crater in Northeast China. Science China Earth Sciences, 56(10): 1629–1638, doi: 10.1007/s11430-013-4695-1

Wang Xiujuan, Wu Shiguo, Dong Dongdong, et al. 2011. Control of mass transport deposits over the occurrence of gas hydrate in Qiongdongnan Basin. Marine Geology and Quaternary Geology (in Chinese), 31(1): 109–118, doi: 10.3724/SP.J.1140.2011.01109

Wei Sihua, Tian Jun. 2022. Mechanisms of greenhouse climate at low atmospheric CO_2 levels in the Late Miocene. Advances in Earth Science (in Chinese), 37(4): 417–428, doi: 10.11867/j.issn.1001-8166.2021.116

Wei Jiangong, Wu Tingting, Zhu Linqi, et al. 2021. Mixed gas sources induced co-existence of sI and sII gas hydrates in the Qiongdongnan Basin, South China Sea. Marine and Petroleum Geology, 128: 105024, doi: 10.1016/j.marpetgeo.2021.105024

Wu Xiaochuan, Pu Renhai, Chen Ying, et al. 2018. Seismic analysis of early-mid Miocene carbonate platform in the southern Qiongdongnan Basin, South China Sea. Acta Oceanologica Sinica, 37(2): 54–65, doi: 10.1007/s13131-017-1128-6

Xie Yuhong, Li Xushen, Fan Caiwei, et al. 2016. The axial channel provenance system and natural gas accumulation of the Upper Miocene Huangliu Formation in Qiongdongnan Basin, South China Sea. Petroleum Exploration and Development, 43(4): 570–578, doi: 10.1016/S1876-3804(16)30067-2

Xie Xinong, Li Sitian, Ge Ligang, et al. 1996. Internal Achitectures and evoluting model of Bay Fan Delta System in Yanan Sag of Qiongdongnan Basin. Acta Sedimentologica Sinica (in Chinese), 41(3): 66–73

Xiong Pengfei, Jiang Tao, Kuang Zenggui, et al. 2021. Sedimentary characteristics and origin of moundes in Meishan Formation, southern Qiongdongnan Basin. Bulletin of Geological Science and Technology (in Chinese), 40(4): 11–21, doi: 10.19509/j.cnki.dzkq.2021.0427

Yang Jiayan, Wu Dexing, Lin Xiaopei. 2008. On the dynamics of the South China Sea Warm Current. Journal of Geophysical Research: Oceans, 113(C8): C08003, doi: 10.1029/2007JC004427

Ye Jianliang, Qin Xuwen, Qiu Haijun, et al. 2018. Data Report: Molecular and isotopic compositions of the extracted gas from China's first offshore natural gas hydrate production test in South China Sea. Energies, English,11(10): 2793, doi: 10.3390/en11102793

Yu Kaiqi, Miramontes E, Alves T M, et al. 2021. Incision of submarine channels over pockmark trains in the South China Sea. Geophysical Research Letters, 48(24): e2021GL092861, doi: 10.1029/2021GL092861

Zhai Puqiang, Chen Honghan, Xie Yuhong, et al. 2013. Modelling of evolution of overpressure system and hydrocarbon migration in deepwater area of Qiongdongnan Basin, South China Sea. Journal of Central South University (Science and Technology) (in Chinese), 44(10): 4187–4201

Zhang Kun, Guan Yongxian, Song Haibin, et al. 2020. A preliminary study on morphology and genesis of giant and mega pockmarks near Andu Seamount, Nansha Region (South China Sea). Marine Geophysical Research, 41(1): 2, doi: 10.1007/s11001-020-09404-y

Zhang Tiansheng, Wu Ziyin, Zhao Dineng, et al. 2019. The morphologies and genesis of pockmarks in the Reed Basin, South China Sea. Haiyang Xuebao (in Chinese), 41(3): 106–120

Zhao Chengbin, Liu Mingjun, Fan Jichang, et al. 2011. High-resolution seismic exploration of Xiuyan impact crater structures. Chinese Journal of Geophysics (in Chinese), 54(6): 1559–1565

Zhao Zhongxian, Sun Zhen, Sun Longtao, et al. 2018. Cenozoic tectonic subsidence in the Qiongdongnan Basin, northern South China Sea. Basin Research, 30(S1): 269–288, doi: 10.1111/bre.12220

Zhu Song, Li Xuejie, Zhang Huodai, et al. 2021. Types, characteristics, distribution, and genesis of pockmarks in the South China Sea: insights from high-resolution multibeam bathymetric and multichannel seismic data. International Geology Review, 63(13): 1682–1702, doi: 10.1080/00206814.2020.1848645